J Bone Miner Metab (2007) 25:383–391
DOI 10.1007/s00774-007-0774-8

ORIGINAL ARTICLE

Ping Zhang · Shigeo M. Tanaka · Qiwei Sun
Charles H. Turner · Hiroki Yokota

Frequency-dependent enhancement of bone formation in murine tibiae and femora with knee loading

Received: April 5, 2007 / Accepted: May 10, 2007

Abstract Knee loading is a relatively new loading modality in which dynamic loads are laterally applied to the knee to induce bone formation in the tibia and the femur. The specific aim of the current study was to evaluate the effects of loading frequencies (in Hz) on bone formation at the site away from the loading site on the knee. The left knee of C57/BL/6 mice was loaded with 0.5 N force at 5, 10, or 15 Hz for 3 min/day for 3 consecutive days, and bone histomorphometry was conducted at the site 75% away from the loading site along the length of tibiae and femora. The results revealed frequency-dependent induction of bone formation, in which the dependence was different in the tibia and the femur. Compared with the sham-loading control, for instance, the cross-sectional cortical area was elevated maximally at 5 Hz in the tibia, whereas the most significant increase was observed at 15 Hz in the femur. Furthermore, mineralizing surface, mineral apposition rate, and bone formation rate were the highest at 5 Hz in the tibia (2.0-, 1.4-, and 2.7 fold, respectively) and 15 Hz in the femur (1.5-, 1.2-, and 1.8 fold, respectively). We observed that the tibia had a lower bone mineral density with more porous microstructures than the femur. Those differences may contribute to the observed differential dependence on loading frequencies.

Key words mechanical loading · knee joint · loading frequency · bone formation · femur · tibia

P. Zhang · Q. Sun · C.H. Turner · H. Yokota (✉)
Department of Biomedical Engineering, Indiana University – Purdue University Indianapolis (IUPUI), Fesler Hall 115, 1120 South Drive, Indianapolis, IN 46202, USA
Tel. +317-274-2448; Fax +317-278-9568
e-mail: hyokota@iupui.edu

P. Zhang · H. Yokota
Department of Anatomy & Cell Biology, Indiana University—Purdue University Indianapolis, IN, USA

S.M. Tanaka
Graduate School of Natural Science and Technology, Kanazawa University, Ishikawa, Japan

Q. Sun · C.H. Turner
Department of Orthopaedic Surgery, Indiana University—Purdue University Indianapolis, IN, USA

Introduction

Physical exercise has been shown to enhance the mechanical strength of bone [1,2], and activities such as swimming [3], climbing [4,5], jumping [6], and whole-body vibration [7] are reported to increase bone mass. These activities are, however, mostly limited to healthy individuals [8], and their efficacy depends on an individual's weight, muscle strength, and fitness level. To understand the mechanism of load-driven bone formation and develop safe and effective load-based therapies, various loading modalities have been investigated [9–13]. One of such modalities is joint loading, which has been recently shown as a unique means to stimulate trabecular and cortical bone formation [14–16]. Knee loading is one form of joint loading that applies lateral loads to synovial joints. The aim of the current study is to evaluate efficacy of knee loading at a site distant from the loading site on the knee and examine any dependence of its anabolic responses on loading frequencies in Hz.

In contrast to most loading modalities such as four-point bending modality [9,10] and axial loading [11–13], joint loading does not depend on load-induced strain at a site of bone formation. Instead, loads are applied laterally to the epiphysis of the synovial joint for induction of bone formation in the diaphysis of long bone. Although its potential anabolic effects have been shown with elbow loading and knee loading, many questions on efficacy as well as loading conditions are unanswered. Here, we addressed a pair of questions: Is knee loading able to induce bone formation in the diaphysis distant from the knee in the tibia as well as in the femur? And if so, is load-driven induction affected by loading frequencies? Although the described loading modality does not provide habitual loads to the knee, its anabolic responses may contribute to strengthening bone and preventing bone loss in individuals who have limited

capabilities of conducting routine exercises such as walking and jogging.

To answer these questions, we conducted a series of loading experiments using mice as a model system. In evaluation of bone formation in the diaphysis away from the knee, we focused on the site 75% distant from the knee in the tibia and the femur along a length of those long bones. Dependence on loading frequencies has been pointed out in previous studies [12,13], but to our knowledge no comparative analysis for the tibia and the femur has been conducted. In addition, although loading frequencies above 10 Hz may occur during daily activities [17], there are few studies that have examined anabolic effects above 10 Hz. Thus, in this report we chose three loading frequencies, at 5, 10, and 15 Hz. Many factors can be involved in dictating frequency responses of the tibia and the femur. In this article, we evaluated potential correlation of porosity and bone mineral density in the tibia and the femur to their frequency responses.

Materials and methods

Experimental animals

Fifty-four female C57/BL/6 mice, ~14 weeks of age (average body weight, ~20 g) were used (Harlan Sprague-Dawley, Indianapolis, IN, USA). Four to five animals were housed per cage and fed with standard laboratory chow and water ad libitum. The animals were allowed to acclimate for 2 weeks before experimentation. All procedures were in accordance with the Institutional Animal Care and Use Committee guidelines.

Mechanical loading

The mouse was placed in an anesthetic induction chamber to induce sedation and mask-anesthetized using 2% isoflurane. The custom-made piezoelectric mechanical loader was employed to apply lateral loads for 3 min/day for 3 consecutive days to the left knee in the lateromedial direction (Fig. 1). The mice were randomly divided into three groups for three loading frequencies (5, 10, or 15 Hz; $n = 8$), and the loads with a peak-to-peak force of 0.5 N were applied. The right hindlimb was used as the sham-loading control. After loading, the mouse was allowed normal cage activity.

Calcein labeling and sample harvest

Mice were given an intraperitoneal injection of calcein (Sigma, St. Louis, MO, USA), a fluorochrome dye, at 30 μg/g body mass on days 2 and 6 after the last loading (Fig. 2). Animals were killed 2 weeks after the last loading, and the left and right femora and tibiae were harvested for micro-computed tomography (μCT) and histomorphometric analyses. The isolated bones were cleaned of soft tissues, and the distal and proximal ends were cleaved to allow infiltration of the fixatives with 10% neutral buffered formalin. After 48 h in the fixatives, bones were transferred to 70% alcohol for storage.

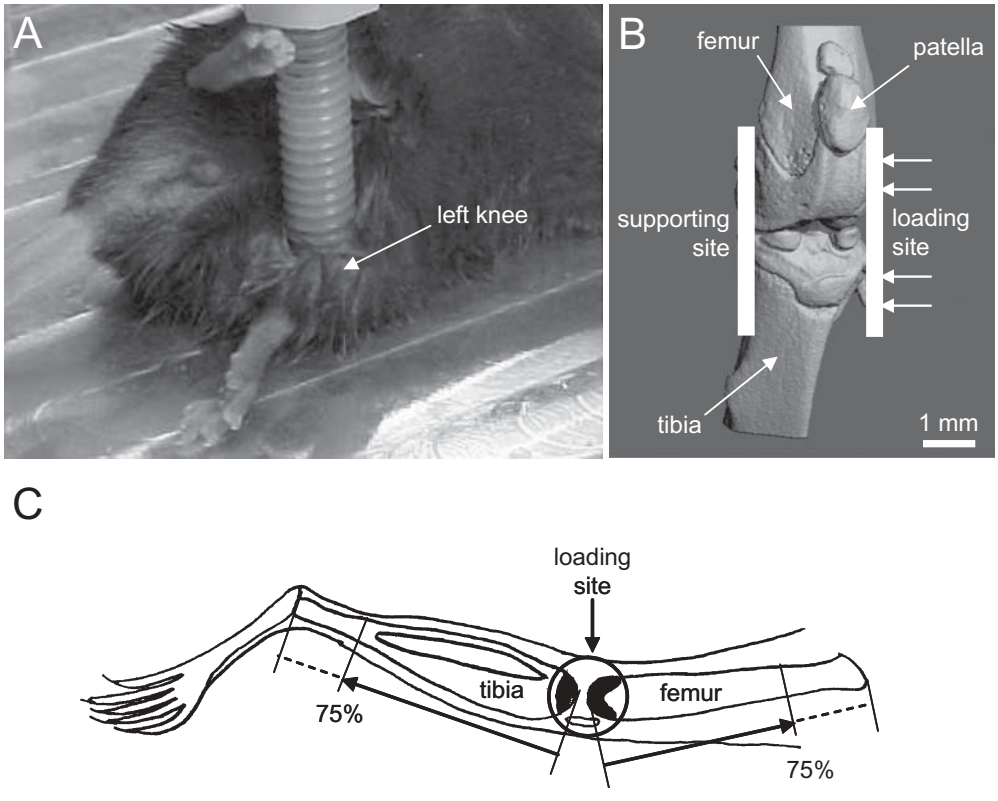

Fig. 1. Setup of the mechanical loader used in this study. **A** Custom-made mechanical loader with a mouse mounted on the table. **B** Micro-computed tomography (μCT) image illustrating the loading site to the tibia and the femur. *Bar* 1 mm. **C** Hindlimb showing the tibial and femoral diaphysis (bone formation site; 75% along the length of the tibia and the femur) and the loading site in the epiphysis

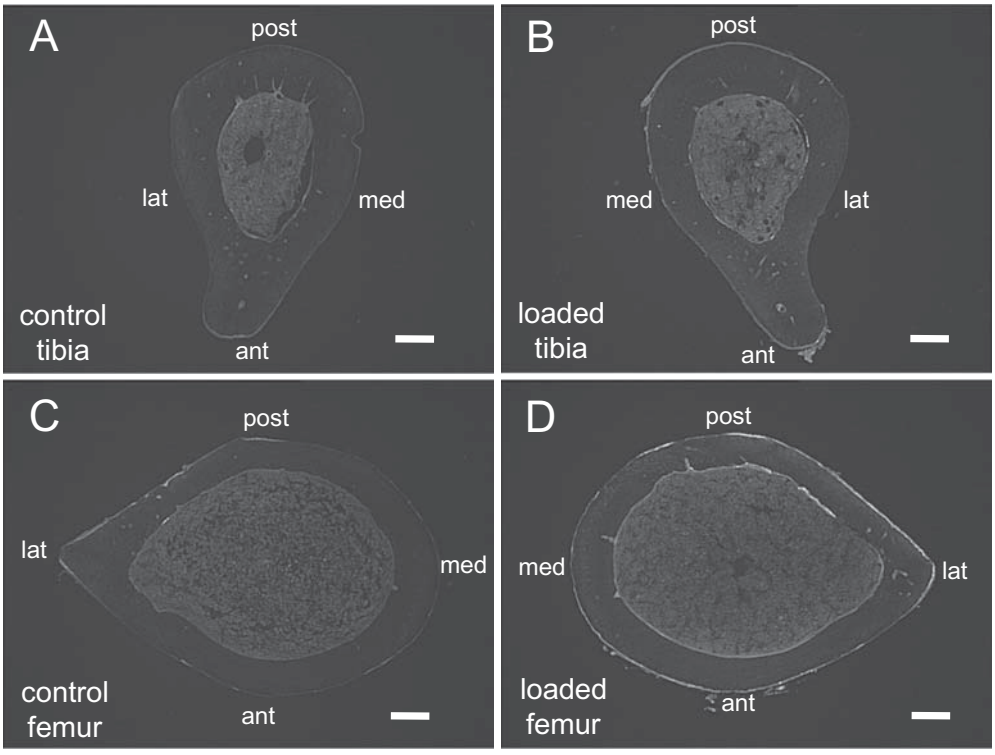

Fig. 2. Tibial and femoral sections. **A** Control tibia. **B** Loaded tibia at 5 Hz. The section was obtained ~12 mm distant from the proximal end of the tibia. **C** Control femur. **D** Loaded femur at 15 Hz. The section was obtained from ~12 mm distant from the distal end of the femur. Medial, *med*; lateral, *lat*; anterior, *ant*; posterior, *post*. *Bars* 200 µm

µCT imaging

Micro-computed tomography was performed using a desktop µCT-20 (Scanco Medical, Auenring, Switzerland) (see Fig. 5). The harvested tibiae and femora were placed in a plastic tube filled with 70% ethanol and centered in the gantry of the machine. A series of cross-sectional images were captured in a 3-mm segment at 30-µm resolution. Bone porosity of the tibial and femoral cortical bone was analyzed [18].

Bone histomorphometry

Specimens were dehydrated in a series of graded alcohols and embedded in methyl methacrylate (Aldrich Chemical, Milwaukee, WI, USA). The transverse sections (~80 µm in thickness) were removed from the tibial shaft, ~12 mm (75%) distant from the proximal end of the tibia, and the femoral shaft, ~12 mm (75%) distant from the distal end of the femur using a diamond-embedded wire saw (Delaware Diamond Knives, Wilmington, DE, USA). After polishing the surface, sections were mounted on standard microscope slides.

We measured total perimeter (B.Pm), endocortical perimeter, single-labeled perimeter (sL.Pm), double-labeled perimeter (dL.Pm), and double-labeled area (dL.Ar). From these measurements, we derived mineralizing surface (MS/BS = [1/2 sL.Pm + dL.Pm]/B.Pm in %), mineral apposition rate (MAR = dL.Ar/dL.Pm/4 in µm/day), and bone formation rate (BFR/BS = MAR × MS/BS × 365 in $\mu m^3/\mu m^2$ per year). To evaluate the effects of loading frequencies, the relative parameters such as rMS/BS, rMAR, and rBFR/BS were derived as differences between the values from the loaded tibiae/femora and the nonloaded control tibiae/femora. The relative alteration was calculated as differences between the loaded (L) and control (C) samples as (L – C)/C × 100 (in %).

To examine load-driven alteration in bone size, the total bone cross-sectional area (mm^2), bone medullary area (mm^2), and cortical thickness (mm) were measured. The cross-sectional cortical area was determined by subtracting the bone medullary area from the total bone cross-sectional area. The cortical thickness was defined as the mean distance between the endosteal surface and the periosteal surface on three sides (medial, lateral, and posterior) for the tibia, or the anterior and posterior sides for the femur. The measurements were taken at the middle of each side, and the mean value was calculated from two independent measurements. We also determined BV/TV (bone area/total area in %) for cortical bone, and relative cortical thickness (cortical bone thickness/cros s-sectional area).

Bone porosity, bone mineral density (BMD), and bone mineral content (BMC)

Intracortical porosity was determined from the tibial and the femoral transverse sections of the nonloaded limbs (n = 24). Using a Nikon Optiphot microscope and a Bioquant digitizing system, we measured cross-sectional cortical area (mm^2), total porous area (mm^2), and the number of pores with areas larger than 11 μm^2. From these measurements, we derived intracortical porosity (ratio of porous area to

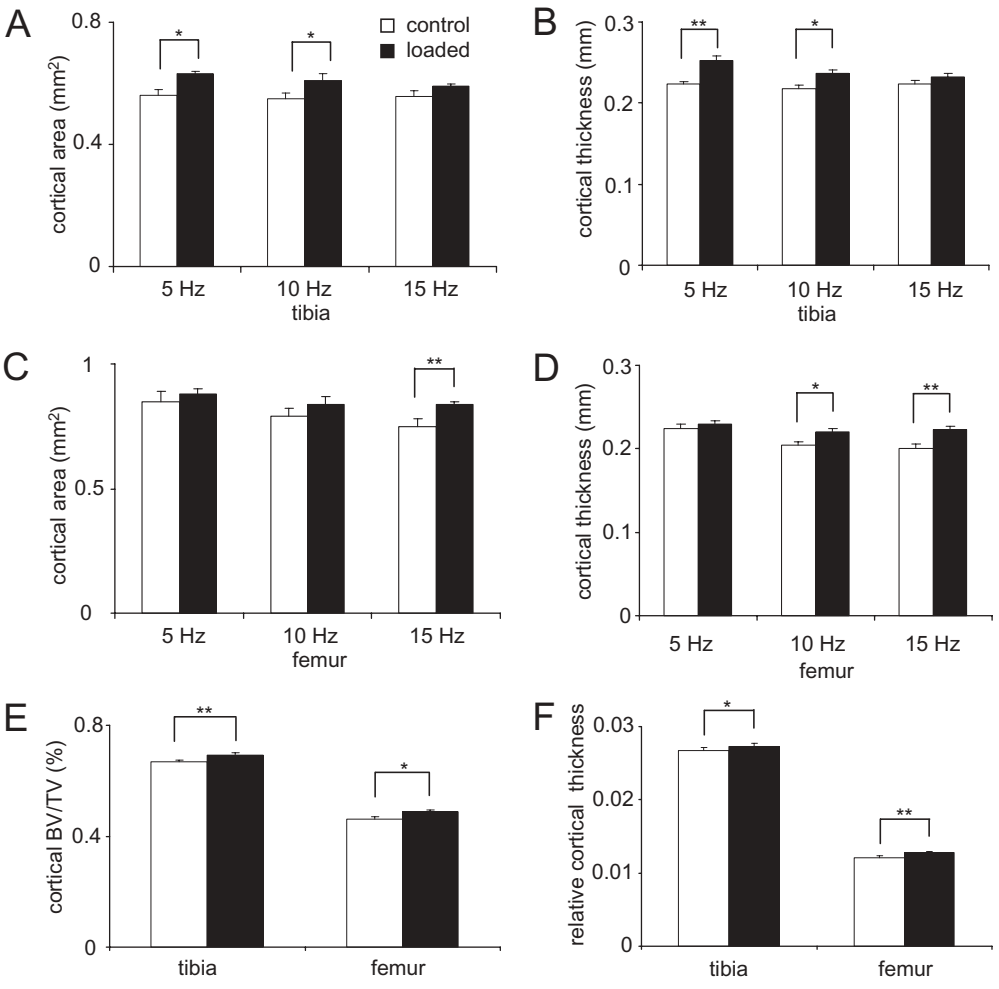

Fig. 3. Alteration in the cross-sectional cortical area and cortical thickness with and without knee loading at 5, 10, and 15 Hz. *Single and double asterisks*, $P < 0.05$ and $P < 0.01$, respectively. **A** Cross-sectional cortical area (mm^2) in the tibia. **B** Cortical thickness (mm) in the tibia. **C** Cross-sectional cortical area (mm^2) in the femur. **D** Cortical thickness (mm) in the femur. **E** Cortical bone volume/total volume (BV/TV) (%) for the tibia and the femur. **F** Relative cortical thickness for the tibia and the femur

total bone area in %) and pore density (number/mm^2). Six age-matched animals were used to determine the BMD and BMC of the entire tibiae and femurs ($n = 12$, including both left and right) with a PIXImus densitometer (software version 1.4x; GE Medical System Lunar, Madison, WI, USA) [19].

Statistical analysis

The data were expressed as mean ± SEM. Statistical significance among groups was examined using one-way analysis of variance (ANOVA), and a post hoc test was conducted using Fisher's protected least significant difference (PLSD) for the pairwise comparisons. A paired *t* test was employed to evaluate statistical significance between the loaded and control samples. All comparisons were two tailed, and statistical significance was assumed for $P < 0.05$.

Results

The animals tolerated the procedures for the loading experiments, and no abnormal behavior including diminished food intake and weight loss was observed. No bruising or other damage was detected at the loading site.

Load-driven alteration in cortical area and cortical thickness in the tibia

A frequency-dependent increase in cortical area and cortical thickness was observed (Fig. 3). The cross-sectional cortical area was increased from 0.56 ± 0.02 mm^2 (control) to 0.63 ± 0.01 mm^2 (loading) at 5 Hz ($P < 0.05$), and from 0.55 ± 0.02 mm^2 (control) to 0.61 ± 0.02 mm^2 (loading) at 10 Hz ($P < 0.05$). No significant alteration was observed at 15 Hz ($P = 0.107$). Similarly, the cortical thickness was elevated from 0.223 ± 0.004 mm (control) to 0.252 ± 0.006 mm (loading) at 5 Hz ($P < 0.01$) and from 0.218 ± 0.004 mm (control) to 0.236 ± 0.005 mm (loading) at 10 Hz ($P < 0.05$). No significant changes were observed at 15 Hz ($P = 0.177$). In the data combined for the three loading groups, the cortical BV/TV increased from 0.667 ± 0.006 (control) to 0.694 ± 0.006 (loading) ($P < 0.01$), and so did the relative cortical thickness, from 0.0265 ± 0.0004 (control) to 0.0277 ± 0.0003 (loading) ($P < 0.05$) (Fig. 3).

Load-driven alteration in cortical area and cortical thickness in the femur

In the femur a frequency response was different from the tibia (Fig. 3). The cortical area was enlarged from 0.75 ± 0.03 mm^2 (control) to 0.84 ± 0.01 mm^2 (loading) with a loading frequency at 15 Hz ($P < 0.01$), but unlike the tibia no significant alteration was observed at 5 Hz ($P = 0.619$) or 10 Hz ($P = 0.189$). The thickness was elevated from 0.201 ± 0.005 mm (control) to 0.223 ± 0.004 mm (loading) at 15 Hz ($P < 0.01$) and from 0.205 ± 0.004 mm (control) to 0.220 ± 0.004 mm (loading) at 10 Hz ($P < 0.05$). No significant changes were observed at 5 Hz ($P = 0.447$). In summary, the cortical BV/TV was increased from 0.461 ± 0.009 (control) to 0.488 ± 0.005 (loading) ($P < 0.05$) in the combined data for the three loading groups. The relative cortical thickness increased from 0.0121 ± 0.0002 (control) to 0.0129 ± 0.0002 (loading) ($P < 0.01$) (Fig. 3). The cross-sectional area of the tibia and the femur was increased with knee loading in all six loading bouts in the present study. However, a statistically significant elevation was observed only in the tibia in response to loads applied at 5 Hz (from 0.83 ± 0.02 mm^2 to 0.90 ± 0.01 mm^2 at $P < 0.05$).

Bone morphometric parameters in the tibia

Bone formation in the periosteal surface was stimulated by knee loading at 5 Hz and 10 Hz (Table 1). Compared to the sham-loading control, loading at 5 Hz resulted in a significant increase in three morphometric parameters (2.0× for MS/BS with $P < 0.01$, 1.4× for MAR with $P < 0.001$, and 2.7× for BFR/BS with $P < 0.01$). Similarly, the loading at 10 Hz elevated these parameters (1.7× for MS/BS with $P < 0.05$, 1.3× for MAR with $P < 0.01$, and 2.1× for BFR/BS with $P < 0.05$). Likewise, bone formation on the endosteal surface was stimulated by knee loading but only at 5 Hz. Compared to the sham-loading control, three morphometric parameters were elevated (1.3× for MS/BS with $P < 0.05$, 1.2× for MAR with $P < 0.01$, and 1.5× for BFR/BS with $P < 0.01$).

Bone morphometric parameters in the femur

Bone formation on the periosteal surface was significantly stimulated by knee loading at 10 and 15 Hz, but no statistical significance was observed on the endosteal surface (Table 2). Compared to the sham-loading control, the loading at 10 Hz elevated two of these parameters on the periosteal surface (1.2× for MAR with $P < 0.05$, and 1.7× for BFR/BS with $P < 0.05$). The loading at 15 Hz was the most effective and resulted in a significant increase in three morphometric parameters (1.5× for MS/BS with $P < 0.05$, 1.2× for MAR with $P < 0.05$, and 1.8× for BFR/BS with $P < 0.05$). No statistical difference was observed with the loading at 5 Hz.

Dependence of anabolic responses on loading frequencies

Dependence on the loading frequencies was prominent in the relative parameters defined on the periosteal surface in the tibia (Fig. 4). Compared to loading at 15 Hz, loading at 5 Hz resulted in a significant increase in three morphometric parameters ($P < 0.01$ for rMS/BS, $P < 0.001$ for rMAR and rBFR/BS). Furthermore, compared to loading at 15 Hz, loading at 10 Hz resulted in an increase in these parameters

Table 1. Bone formation with the loading frequencies at 5–15 Hz in the tibia

	MS/BS (%)	*P* value	MAR (μm/day)	*P* value	BFR/BS (μm^3/μm^2/year)	*P* value
At 5 Hz						
Periosteum						
Control	11.15 ± 1.40	<0.01	0.20 ± 0.01	<0.001	8.13 ± 1.30	<0.01
Knee loading	21.79 ± 2.51		0.27 ± 0.01		21.64 ± 2.78	
Endosteum						
Control	12.34 ± 1.07	<0.05	0.20 ± 0.01	<0.01	9.05 ± 0.95	<0.01
Knee loading	16.23 ± 1.13		0.23 ± 0.01		13.92 ± 1.18	
At 10 Hz						
Periosteum						
Control	11.34 ± 2.65	<0.05	0.21 ± 0.01	<0.01	8.80 ± 2.16	<0.05
Knee loading	18.84 ± 2.20		0.26 ± 0.01		18.32 ± 2.56	
Endosteum						
Control	11.81 ± 2.80	NS	0.20 ± 0.01	NS	8.40 ± 1.89	NS
Knee loading	14.87 ± 3.24		0.23 ± 0.01		12.00 ± 2.55	
At 15 Hz						
Periosteum						
Control	10.16 ± 1.55	NS	0.20 ± 0.01	NS	7.63 ± 1.34	NS
Knee loading	13.91 ± 2.31		0.22 ± 0.01		11.46 ± 2.12	
Endosteum						
Control	11.57 ± 1.09	NS	0.20 ± 0.01	NS	8.48 ± 0.99	NS
Knee loading	14.12 ± 1.52		0.22 ± 0.01		11.32 ± 1.52	

MS, mineralizing surface; BS, bone surface; MAR, mineral apposition rate; BFR, bone formation rate
NS, $P > 0.05$

Table 2. Bone formation with the loading frequencies at 5–15 Hz in the femur

	MS/BS (%)	*P* value	MAR (μm/day)	*P* value	BFR/BS ($\mu m^3/\mu m^2$/year)	*P* value
At 5 Hz						
Periosteum						
Control	12.42 ± 1.06	NS	0.17 ± 0.01	NS	7.98 ± 0.82	NS
Knee loading	14.20 ± 0.75		0.19 ± 0.01		9.91 ± 0.74	
Endosteum						
Control	13.35 ± 1.01	NS	0.19 ± 0.01	NS	9.31 ± 0.67	NS
Knee loading	14.88 ± 1.47		0.20 ± 0.01		11.13 ± 1.22	
At 10 Hz						
Periosteum						
Control	13.11 ± 1.00	NS	0.18 ± 0.01	<0.05	8.57 ± 0.86	<0.05
Knee loading	17.60 ± 2.30		0.21 ± 0.01		14.15 ± 2.45	
Endosteum						
Control	11.77 ± 2.56	NS	0.19 ± 0.01	NS	8.07 ± 1.86	NS
Knee loading	13.52 ± 2.43		0.20 ± 0.01		10.61 ± 2.61	
At 5 Hz						
Periosteum						
Control	13.10 ± 1.80	<0.05	0.18 ± 0.01	<0.05	8.60 ± 1.23	<0.05
Knee loading	19.32 ± 1.85		0.22 ± 0.01		15.50 ± 2.03	
Endosteum						
Control	13.42 ± 1.15	NS	0.18 ± 0.01	NS	8.86 ± 0.74	NS
Knee loading	15.99 ± 1.32		0.20 ± 0.01		11.67 ± 1.10	

NS, $P > 0.05$

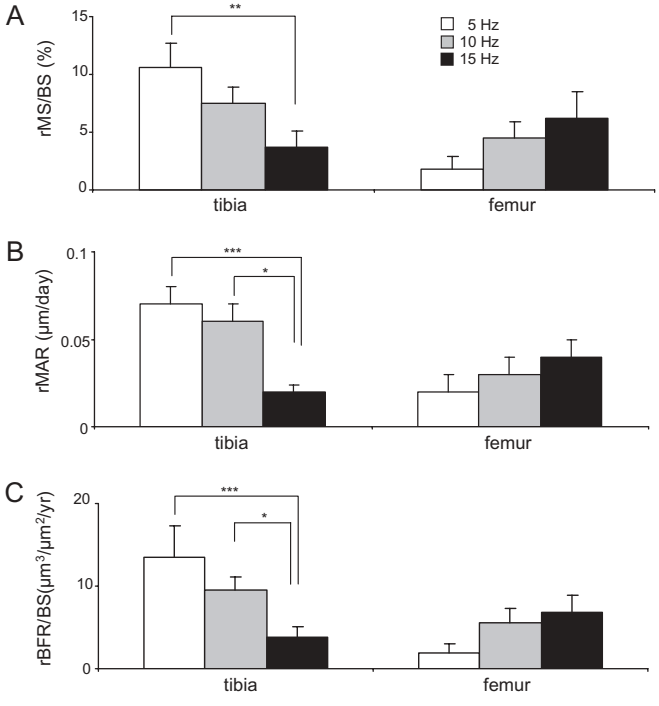

Fig. 4. Alteration in the relative histomorphometric parameters on the periosteal and endosteal surfaces with knee loading at 5, 10, and 15 Hz. *Single, double, and triple asterisks*, $P < 0.05$, $P < 0.01$, and $P < 0.001$, respectively. **A** Relative mineralizing surface/bone surface (MS/BS, %). **B** Relative mineral apposition rates (MAR, μm/day). **C** Relative bone formation rate (BFR)/BS ($\mu m^3/\mu m^2$/year)

($P < 0.05$ for rMAR and rBFR/BS). In contrast to the periosteal surface in the tibia, no significant loading effects were observed in the femur regarding those morphometric parameters ($P = 0.11$–0.19; data not shown).

To further examine the effects of knee loading on the periosteal surfaces in the tibia, rMS/BS, rMAR, and rBFR/BS were determined and normalized by the values of the control group (% of control). Based on the normalized change on the periosteal surface, loading at 5 Hz elevated rMAR ($P < 0.001$) and rBFR/BS ($P < 0.01$) more than loading at 15 Hz did. Furthermore, loading at 10 Hz resulted in a significant increase in rMAR and rBFR/BS (both, $P < 0.05$) compared to loading at 15 Hz. In comparison to the periosteal surface in the tibia, no significant loading effects were observed in the femur for the morphometric parameters ($P = 0.20$–0.29; data not shown). Among the three frequencies employed in the study, in the tibia bone formation was most enhanced at the lowest frequency (5 Hz) whereas in the femur it was most effective at the highest frequency (15 Hz).

Bone porosity, BMD, and BMC

To evaluate any link of the observed frequency dependence to bone microstructure, we evaluated bone porosity as well as BMD and BMC. First, bone porosity in the cortical bone was significantly different between the tibia and femur (Fig. 5). The measurement of intracortical porosity revealed that the tibia (1.79% ± 0.10%) was more porous than the femur (1.18% ± 0.04%) ($P < 0.001$). Similarly, the porosity density (number/mm^2) was higher in the tibia (831 ± 42) than the femur (666 ± 20) ($P < 0.01$). Those observations were confirmed by μCT images, in which the tibia presented the greater number of pores and more porous areas than the femur. Second, in age-matched mice the value of BMD in the tibia (32.3 ± 0.7 mg/cm^2) was significantly lower than that in the femur (34.8 ± 0.5 mg/cm^2) ($P < 0.01$). In the BMC

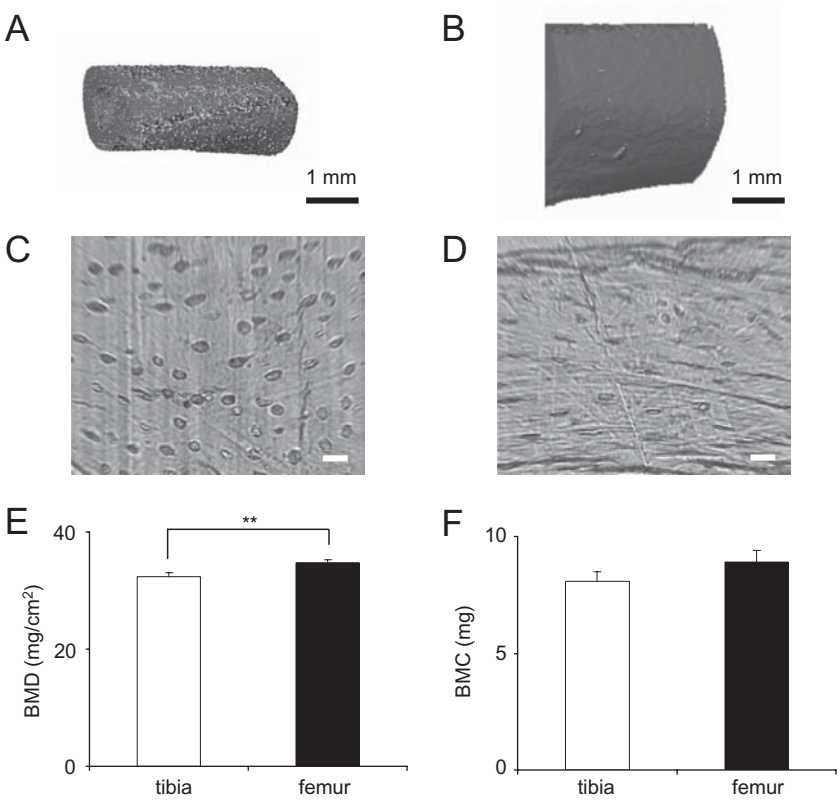

Fig. 5. Bone porosity in the tibia and the femur. **A** Three-dimensional (3-D) reconstruction of μCT image of tibia. **B** 3-D reconstruction of μCT image of femur. **C** Tibial cross section with pores. **D** Femoral cross section with pores. **E** Bone mineral density (BMD) for the tibia and the femur. **F** Bone mineral content (BMC) for tibia and femur. *Bars* **A**, **B** 20 μm

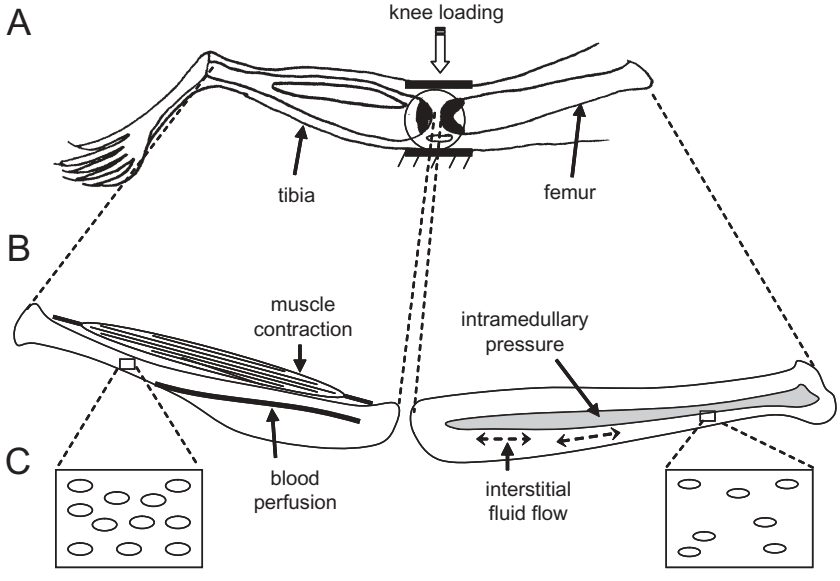

Fig. 6. Potential contributors to the enhancement of bone formation in the femur with knee loading. This schematic illustration includes alteration in intramedullary pressure, muscle contraction, activation of blood perfusion, and load-driven interstitial fluid flow

measurement, although the value in the tibia (8.1 ± 0.4 mg) was lower than in the femur (8.9 ± 0.5 mg), no statistical significance was detected ($P > 0.05$).

Discussion

The present study reveals that knee loading induces formation of cortical bone on the periosteal and endosteal surfaces at a location considerably remote from the loading site. As a mechanism of induction of bone formation, we postulate that low-magnitude loads applied to the epiphysis alter pressure in the intramedullary cavity and this in turn influences intracortical fluid flow (Fig. 6) [20–24]. To examine possible induction of molecular transport with knee loading, we previously examined load-driven molecular transport using a fluorescence recovery after photobleaching technique [25]. In the experiment, a lacuna in the diaphysis was photo bleached, and a time constant for

recovering fluorescence signals was determined with and without knee loading. The results revealed that knee loading shortened the time constant. Furthermore, oscillatory alteration of intramedullary pressure in the femur was observed in response to sinusoidal loading with knee loading [26]. Taken together, knee loading appears to affect motion of interstitial fluid as well as medullary fluid.

The loading effects were dependent on loading frequencies, and the dependence was different in the tibia and the femur. In the tibia, 5 and 10 Hz was more effective than 15 Hz, whereas in the femur induction was most significant at 15 Hz. Other studies indicate that the effective frequency differs depending on the loading modalities [17,27,28]. In whole-body vibration, higher frequencies (>30 Hz) have been suggested to be more effective [29,30]. Similarly, with ulna axial loading using rats, bone formation was increasingly elevated with an increase in loading frequencies from 1 to 10 Hz [28]. In contrast, with ulna axial loading using mice, the frequencies at 5 and 10 Hz were reported to be more effective than 20 or 30 Hz [12].

A potential cause of differential frequency responses in the current study includes differences in transmission of force in the knee, size and shape of tibiae and femora, blood pressure and pressure in the lacunocanalicular network, viscoelastic characters, cellular and molecular environments, and microstructures such as porosity. As the studies by Qin et al. have shown that the rate of bone formation is correlated to a distribution of pores in a cross section of turkey ulnae [31,32], we examined porosity of cortical bone of the tibia and the femur. Histological and μCT analyses revealed that cortical bone in the femur has a higher BMD with fewer pores than the tibia. According to a poroelasticity theory, the observed difference in the pore volume fraction alters permeability of solutes in the lacunocanalicular network, compressibility of the poroelastic medium, and bulk modulus of the undrained poroelastic bone [33,34]. The difference should thereby affect nutrient transport, bone mineralization, and mechanotransduction. We observed that the tibia with a high pore fraction was responsive to a lower loading frequency than the femur. Further investigation is necessary to evaluate the linkage between porosity and frequency dependence in the tibia and the femur.

Porosity is directly linked to the size of the osteocyte population, which influences activities in bone remodeling. Recent studies have suggested that the relationship between osteocyte density and bone formation rate varies depending on skeletal site and developmental history. In human cancellous bone, an inverse relationship between osteocyte density and bone formation rate was reported [35], whereas in rat woven bone osteocytes were viewed as a local initiator of bone remodeling and remodeling at an accelerated rate was observed at high lacunar density [36]. Between the tibia and the femur in the present study, the tibia exhibited a higher bone formation rate at 5 and 10 Hz and the femur at 15 Hz. Our results suggest that any relationship between osteocyte density and bone formation rate is apparently dependent on a loading condition.

The present study presented differential sensitivity of the periosteal and endosteal surfaces in response to knee loading. We observed increased bone formation in the periosteum and the endosteum, but in contrast to the marked enhancement of bone formation on the periosteal surface, the endosteal surface exhibited no statistically significant increase except for the bout in the tibia at 5 Hz. Interestingly, the observations herein are consistent with some of the previous studies using other loading modalities such as axial loading [37,38], bending [39], climbing [5], running [40], and jumping [6]. The results may suggest a differential role of load-driven alterations in intramedullary pressure between the periosteal and endosteal surfaces. Alternatively, differences in anatomical and physiological microenvironments exist, and differential anabolic responses could result from variations in cellular and molecular compositions as well as in heterogeneous propagation of load-driven pressure gradients and interstitial fluid flow.

In summary, the current study demonstrates that knee loading is an effective means to induce bone formation in the proximal diaphysis in the femur and the distal diaphysis in the tibia. Knee loading is a recently developed loading modality that could, with further research, provide potential for slowing bone loss in the femur and the tibia. Understanding the mechanism of bone formation with knee loading could contribute to future treatments and therapies for the promotion of bone quality.

Acknowledgments The authors appreciate G.M. Malacinski for critical reading of the manuscript. This study was in part supported by NIH R03AG024596 and NIH R01AR52144. The authors have no conflict of interest.

References

1. Holy X, Zerath E (2000) Bone mass increases in less than 4 wk of voluntary exercising in growing rats. Med Sci Sports Exerc 32:1562–1569
2. Turner CH, Robling AG (2005) Mechanisms by which exercise improves bone strength. J Bone Miner Metab 23:S16–S22
3. Hart KJ, Shaw JM, Vajda E, Hegsted M, Miller SC (2001) Swim-trained rats have greater bone mass, density, strength, and dynamics. J Appl Physiol 91:1663–1668
4. Notomi T, Okimoto N, Okazaki Y, Tanaka Y, Nakamura T, Suzuki M (2001) Effects of tower climbing exercise on bone mass, strength, and turnover in growing rats. J Bone Miner Res 16:166–171
5. Mori T, Okimoto N, Sakai A, Okazaki Y, Nakura N, Notomi T, Nakamura T (2003) Climbing exercise increases bone mass and trabecular bone turnover through transient regulation of marrow osteogenic and osteoclastogenic potentials in mice. J Bone Miner Res 18:2002–2009
6. Kodama Y, Umemura Y, Nagasawa S, Beamer WG, Donahue LR, Rosen CR, Baylink DJ, Farley JR (2000) Exercise and mechanical loading increase periosteal bone formation and whole bone strength in C57BL/6J mice but not in C3H/Hej mice. Calcif Tissue Int 66:298–306
7. Flieger J, Karachalios T, Khaldi L, Raptou P, Lyritis G (1998) Mechanical stimulation in the form of vibration prevents postmenopausal bone loss in ovariectomized rats. Calcif Tissue Int 63:510–514
8. Chestnut CH (1993) Bone mass and exercise. Am J Med 95: 34S–36S
9. Pedersen EA, Akhter MP, Cullen DM, Kimmel DB, Recker RR (1999) Bone response to in vivo mechanical loading in C3H/HeJ mice. Calcif Tissue Int 65:41–46
10. Kameyama Y, Hagino H, Okano T, Enokida M, Fukata S, Teshima R (2004) Bone response to mechanical loading in adult rats with collagen-induced arthritis. Bone (NY) 35:948–956

11. Li J, Burr DB, Turner CH (2002) Suppression of prostaglandin synthesis with NS-398 has different effects on endocortical and periosteal bone formation induced by mechanical loading. Calcif Tissue Int 70:320–329
12. Warden SJ, Turner CH (2004) Mechanotransduction in cortical bone is most efficient at loading frequencies of 5–10 Hz. Bone (NY) 34:261–270
13. Hsieh YF, Robling AG, Ambrosius WT, Burr DB, Turner CH (2001) Mechanical loading of diaphyseal bone in vivo: the strain threshold for an osteogenic response varies with location. J Bone Miner Res 16:2291–2297
14. Tanaka SM, Sun HB, Yokota H (2004) Bone formation induced by a novel form of mechanical loading on joint tissue. Biol Sci Space 18:41–44
15. Yokota H, Tanaka SM (2005) Osteogenic potential with joint loading modality. J Bone Miner Metab 23:302–308
16. Zhang P, Tanaka SM, Jiang H, Su M, Yokota H (2006) Diaphyseal bone formation in murine tibiae in response to knee loading. J Appl Physiol 100:1452–1459
17. Turner CH, Yoshikawa T, Forwood MR, Sun TC, Burr DB (1995) High frequency components of bone strain in dogs measured during various activities. J Biomech 28:39–44
18. Jove G, Michael R, Lisa P (2003) Effect of bone porosity on the mechanical integrity of the bone–cement interface. J Bone Joint Surg [Am] 85:1901–1908
19. Alam I, Warden SJ, Robling AG, Turner CH (2005) Mechanotransduction in bone does not require a functional cyclooxygenase-2 (COX-2) gene. J Bone Miner Res 20:438–446
20. Burr DB, Robling AG, Turner CH (2002) Effects of biomechanical stress on bones in animals. Bone (NY) 30:781–786
21. Knothe Tate ML, Knothe U (2000) An ex vivo model to study transport processes and fluid flow in loaded bone. J Biomech 33:247–254
22. Tami AE, Nasser P, Verborgt O, Schaffler MB, Knothe Tate ML (2002) The role of interstitial fluid flow in the remodeling response to fatigue loading. J Bone Miner Res 17:2030–2037
23. Montgomery RJ, Sutker BD, Bronk JT, Smith SR, Kelly PJ (1988) Interstitial fluid flow in cortical bone. Microvasc Res 35:295–307
24. Warden SJ (2006) Breaking the rules for bone adaptation to mechanical loading. J Appl Physiol 100:1441–1442
25. Su M, Jiang H, Zhang P, Liu Y, Wang E, Hsu A, Yokota H (2006) Knee-loading modality drives molecular transport in mouse femur. Ann Biomed Eng 34:1600–1606
26. Zhang P, Su M, Liu Y, Hsu A, Yokota H (2007) Knee loading dynamically alters intramedullary pressure in mouse femora. Bone (NY) 40:538–543
27. Rubin CT, McLeod KJ (1994) Promotion of bony ingrowth by frequency-specific, low-amplitude mechanical strain. Clin Orthop Relat Res 298:165–174
28. Hsieh YF, Turner CH (2001) Effects of loading frequency on mechanically induced bone formation. J Bone Miner Res 16: 918–924
29. Rubin C, Turner AS, Bain S, Mallinckrodt C, McLeod KA (2001) Low mechanical signals strengthen long bones. Nature (Lond) 412:603–604
30. Rubin C, Recker R, Cullen D, Ryaby J, McCabe J, McLeod K (2004) Prevention of postmenopausal bone loss by a low-magnitude, high-frequency mechanical stimuli: a clinical trial assessing compliance, efficacy, and safety. J Bone Miner Res 19: 343–351
31. Qin YX, Kaplan T, Saldanha A, Rubin CT (2003) Fluid pressure gradients, arising from oscillations in intramedullary pressure, is correlated with the formation of bone and inhibition of intracortical porosity. J Biomech 36:1427–1437
32. Qin YX, Lin W, Rubin C (2002) The pathway of bone fluid flow as defined by in vivo intramedullary pressure and streaming potential measurements. Ann Biomed Eng 30:693–702
33. Cowin SC (1999) Bone poroelasticity. J Biomech 32:217–238
34. Swan CC, Lakes RS, Brand RA, Stewart KJ (2003) Micromechanically based poroelastic modeling of fluid flow in Haversian bone. J Biomech Eng 125:25–37
35. Qiu S, Rao DS, Palnitkar S, Parfitt AM (2002) Relationships between osteocyte density and bone formation rate in human cancellous bone. Bone (NY) 31:709–711
36. Hernandez CJ, Majeska RJ, Schaffler MB (2004) Osteocyte density in woven bone. Bone (NY) 35:1095–1099
37. Lee KC, Maxwell A, Lanyon LE (2002) Validation of a technique for studying functional adaptation of the mouse ulna in response to mechanical loading. Bone (NY) 31:407–412
38. De Souza RL, Matsuura M, Eckstein F, Rawlinson SC, Lanyon LE, Pitsillides AA (2005) Non-invasive axial loading of mouse tibiae increases cortical bone formation and modifies trabecular organization: a new model to study cortical and cancellous compartments in a single loaded element. Bone (NY) 37:810–818
39. LaMothe JM, Hamilton NH, Zernicke RF (2005) Strain rate influences periosteal adaptation in mature bone. Med Eng Phys 27:277–284
40. Wu J, Wang XX, Higuchi M, Yamada K, Ishimi Y (2004) High bone mass gained by exercise in growing male mice is increased by subsequent reduced exercise. J Appl Physiol 97:806–810